Safety and Risk Mitigation in Emerging Urban Mobility: A Study on Head Trauma and Helmet Effectiveness for Personal Electric Vehicles

Caroline Deck, Nicolas Bourdet, Frank Meyer

Abstract New personal mobility devices, such as handlebar-less gyropods and e-scooters, provide eco-friendly transportation options but also present significant safety concerns, particularly regarding head injuries sustained during accidents. Given the lack of helmet regulations and available injury statistics, this study investigates virtual accident scenarios to assess head injury risks and advocate for helmet use to improve safety in urban mobility. A total of 432 multibody simulations were conducted to assess head impact conditions during falls involving emerging electric vehicles (EEVs), followed by finite element simulations using the SUFEHM head model. The results showed a high risk of skull fractures and neurological injuries in unhelmeted users, with risks exceeding 90% in most cases and even at lower speeds. Helmet use significantly reduced these risks—by approximately 65% for skull fractures and 75% for brain injuries—highlighting its critical role in improving EEV safety across all user types. By quantifying these risks prior to accidents, this study aims to provide key insights for policymakers and raise awareness among users.

Keywords Emergency Electric Vehicle, head injury risk assessment, helmet efficiency, kinematic analysis, virtual fall simulations.

I. INTRODUCTION

The emergence of new personal mobility devices—commonly referred to as emerging electric vehicles (EEVs)—such as handlebar-less gyropods, single-wheelers, and electric scooters, has raised several safety challenges for users. The French Road Safety department reported 44 e-mobility users killed in 2023 (34 more than in 2019), and the estimated number of injured (three-quarters in urban areas) increased from 158 to 671 in the same period, which is a four-fold increase [1]. As the use of these devices increases, it is crucial for both public authorities and users to understand the potential injury risks associated with them, particularly the benefits of wearing helmets. Over recent years, urban mobility patterns worldwide have been significantly altered by the rise of micromobility vehicles. Among these, bicycles remain the most commonly used mode of transport, followed by stand-up electric scooters (e-scooters) [2]. The growth of e-scooter use has outpaced other modes, largely due to the minimal physical effort required, which enhances their potential to replace or complement traditional transportation modes, such as public transit and cars, for longer trips [3]. These new mobility options allow users to travel at speeds ranging from 6 km/h to 40 km/h, offering a viable solution to the growing issues of congestion and pollution in urban environments. More compact and lightweight than bicycles, these devices – once perceived as recreational – are now being adopted as legitimate modes of transport, like bicycles. Despite the enthusiasm surrounding these innovations, experts in accident analysis and biomechanics have raised concerns about safety risks, particularly regarding head injuries resulting from falls or accidents. Notably, helmet use is not mandatory for many of these emerging modes of transportation, and comprehensive data on falls, hospitalisations, and injury characteristics remain scarce. In particular, there is a lack of detailed information regarding accident scenarios, victim characteristics (e.g., weight, height), ground surface properties, helmet usage and type, helmet damage assessment, and whether victims suffered long-term physical or psychological consequences. This study aims to examine virtual accident scenarios involving EEVs to better understand the associated injury risks and the role of helmets in mitigating these risks.

Head and facial injuries are the most common types of injury for micromobility users involved in collisions [4]. Therefore, understanding the kinematic responses of users during crashes is critical for studying injury

C. Deck (e-mail: deck@unistra.fr; tel: +33 368852940), N. Bourdet and F. Meyer are Researchers at Strasbourg University (UNISTRA), The Engineering science, computer science and imaging laboratory, ICube UMR 7357 CNRS, Strasbourg, France.

mechanisms and establishing safety standards. However, collecting kinematic data directly from traffic crash sites is challenging, and such data are often not included in accident statistics. As an alternative to traditional epidemiological studies, this research reconstructs typical crashes involving micromobility users using simulation tools like multibody software. These simulation technologies have been used extensively in traffic safety research to study the effects of different variables on the dynamic response of vulnerable road users, such as vehicle types, collision types, and collision speeds.

Most existing research has focused on bicycles and electric bicycles, with relatively few studies addressing the consequences of crashes involving other micromobility devices [5–6]. For example, [7] used the MADYMO platform to numerically simulate four types of vehicle-to-road user collisions, including those involving single-wheel, two-wheel, and bicycle devices.

Vehicle speed is a key factor influencing the severity of head injury risk for vulnerable road users (VRUs). However, the specific influence of rider speed in single-vehicle emerging electric vehicle (EEV) accidents—particularly at higher speeds—remains underexplored. In [8], rider speed was divided into five levels ranging from 4 to 18 km/h. Injury metrics were evaluated using global kinematic head injury criteria and the THUMS maximum principal strain metric across various impact scenarios and speeds. However, that study did not account for helmet use.

Several studies have also focused specifically on e-scooter crashes. For instance, [9] used MADYMO to simulate e-scooter falls caused by potholes, reporting an average head impact speed of approximately 6.3 m/s, with all impacts occurring at oblique angles. However, neither head injury risks nor helmet benefits were assessed. Similarly, [10] simulated e-scooter collisions with vehicles and reported head linear accelerations ranging from 30 g to 80 g, but without evaluating injury risks or helmet effectiveness.

[11] investigated side-impact motor vehicle collisions involving micromobility vehicles—including bicycles and e-scooters—using PC-Crash simulations. Results indicated that bicycles offered better protection in side-impact scenarios compared to e-scooters, as cyclists experienced lower HIC15 values when vehicle impact speed exceeded 30 km/h.

In another study, [12] developed and validated a finite element (FE) model to simulate 27 fall scenarios resulting from curb collisions. Head–ground impact forces and velocities were analysed with and without helmets, although no explicit head injury risk metrics were computed.

A multibody model of e-scooter falls caused by wheel–curb collisions was developed and compared with experimental crash tests by [13]. A total of 162 scenarios were simulated to assess the influence of fall conditions—such as initial speed, inclination, obstacle orientation, and user size—on head impact kinematics. In 44% of simulations, the forehead was the first point of contact. The average tangential and normal impact speeds were 3.5 m/s and 4.8 m/s, respectively. Although preliminary data were provided for protective equipment design, no direct head injury risk assessment was performed.

In summary, while EEVs such as handlebar-less gyropods and e-scooters offer sustainable alternatives for urban transport, they also introduce significant safety concerns, particularly in relation to head trauma during falls or collisions. Given the current lack of detailed head injury risk assessments in single-vehicle EEV accidents, as well as limited data on helmet usage and injury prevalence, the present study aims to fill these gaps. It uses virtual accident simulations to identify key injury risks and quantitatively evaluate the protective benefits of helmet use across various crash configurations, for both adult and 6–10-year-old users.

II. METHODS

This paper presents a parametric study-based methodology to evaluate head impact conditions in terms of impact areas and velocities in single-user falls involving Emerging Electric Vehicles (EEVs). The analysis focuses first on the head's initial orientation and velocity just before contact. In the next step, head injury risks are assessed by simulating head impacts on the ground using the Strasbourg University Finite Element Head Model (SUFEHM), a human head FE model developed at Strasbourg University. Simulations are conducted both with and without a bicycle helmet to quantify the protective benefits of helmet use.

Kinematic analysis of EEV users

The kinematic analysis of EEV users was performed using Madymo®, a multibody simulation software widely employed for occupant safety assessments. Unlike FE models, where contact between bodies is defined by surface deformation, multibody simulations rely on penetration functions that express force as a function of displacement. This approach significantly reduces computation time, enabling the simulation of numerous accident scenarios.

The HBM used in this study is the pedestrian model developed by TNO, integrated into Madymo® and referenced in works by [14]. This model comprises 64 ellipsoids connected by 52 rigid bodies, linked through various kinematic joints, including spherical and translational-revolution joints. The reference model represents an "average" adult with a height of 1.75 m and a mass of 73 kg, with inertial properties based on the study by [15]. The stiffness values at the joints are derived from experimental tests on volunteers and cadavers.

To account for different user profiles, the adult model was scaled to represent children aged 10 years and 6 years, with respective heights of 137 cm and 116 cm and masses of 35 kg and 21 kg. This scaling was performed using the GEBOD tool and database, available in Madymo®, as proposed by [16] and [17]. Figure 1 provides an illustration of the three user models considered in this study.

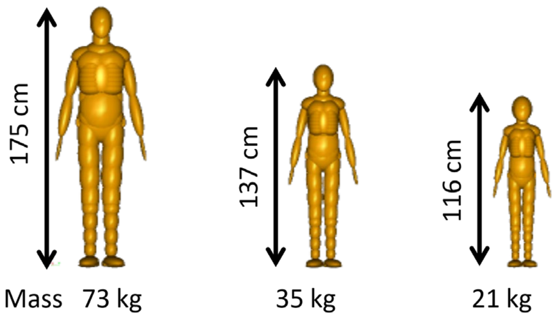

Fig. 1. Illustration of the multibody model of the human body, for an average adult (1.75 m, 73 kg), for a 10-year-old child (1.37 m, 35 kg) and for a 6-year-old child (1.16 m, 21 kg), used for multibody model simulations.

Three types of Emerging Electric Vehicle (EEV) were developed for this study: the handlebar-less gyropod; the electric single-wheel; and the electric scooter.

- The handlebar-less gyropod, commonly referred to as an electric skateboard, E-board, or hoverboard, typically features two side-by-side wheels with small platforms in between for the user to stand on. Two variants of this gyropod have been developed, one with 6.5 inch diameter wheels (60x20 cm) and the second model with 10 inch diameter wheels (70x30 cm).
- The electric single-wheel, also known as an electric unicycle, gyro, or E-wheel, is a key innovation that has contributed to the popularity of gyroscopic vehicles. This device features a faired wheel equipped with sensors, a gyroscopic motor, two retractable footrests, and a rechargeable battery. Similar to the gyropod, two versions of the electric unicycle have been developed, one with a wheel diameter of 14 inches (35x33 cm) and the other with a wheel diameter of 18 inches (45x35 cm).
- Finally, the third category of EEV studied is the electric scooter, or e-scooter. Two models of this mode of transport were also designed, the scooter with 5.5 inch diameter wheels and with 10 inch diameter wheels.

The geometries and masses of these models were designed based on real-world EEVs available on the commercial market. Each component of the frame was modelled as a rigid body, incorporating mass and inertia, and connected through kinematic joints. The wheel is not rigidly attached to the chassis; it is free to rotate around its axis. In the case of the e-scooter, the front wheel is mounted on a pivot, allowing it to turn, and the handlebar is connected to this wheel, enabling steering motion.

In the case of EEVs, the wheels are typically harder—made of rubber or polyurethane—and non-pneumatic, resulting in a smaller contact patch with the ground. Consequently, the wheel–road interaction is modelled using a friction coefficient of 0.7 for dry surfaces and a normal contact stiffness of 3.0×10^6 N/m, based on values provided in the MADYMO Reference Manual and established tire–road interaction models [31]. An illustration of the developed model as well as mass and inertia implemented is shown in Fig. 2.

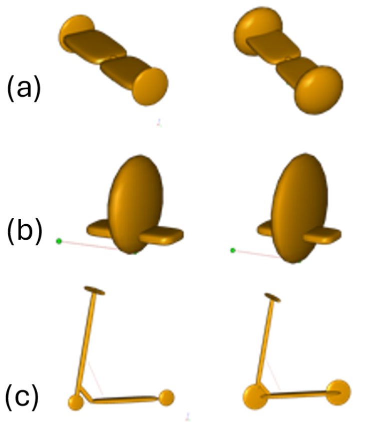

(d)

EmergingElectric Vehicles	Mass [kg]	IXX $[kgm^2]$	IYY $[kgm^2]$	IZZ $[kgm^2]$
Hoverboad-6.5-inch	18.80	2.56	2.02	2.56
Hoverboad-10-inch	20.80	2.57	2.03	2.57
Single-wheel-14-inch	16.50	2.01	2.02	2.01
Single-wheel-18-inch	18.20	2.02	2.03	2.02
E-scooter-5.5-inch	14.00	0.71	2.42	1.72
E-scooter-10-inch	16.00	0.72	2.43	1.73

Fig. 2. Illustration of multibody models of (a) gyropod, (b) single-wheel and (c) e-scooter, as well as (d) mass and inertia implemented.

Four virtual fall configurations were analysed:

- Rear imbalance for the gyropod and mono-wheel.
- Lateral imbalance for the electric scooter.
- Falls caused by pavement deterioration, such as encountering a hole.
- Impacts against a curb, considering two approach angles: perpendicular and 45°.

Regarding the speeds of the EEVs at the time of the "accident", simulations were conducted at speeds ranging from 5 km/h to 30 km/h in 5 km/h increments, resulting in six speed conditions per EEV and per user. Figure 3 schematically summarises the parameters studied during the simulation of falls involving EEV users, the six speed configurations, the four fall configurations, the three types of EEV, and the three user profiles. In total, 432 virtual fall simulations were conducted and analysed in terms of head impact point location as well as angle and velocities of the head just before its impact on the ground.

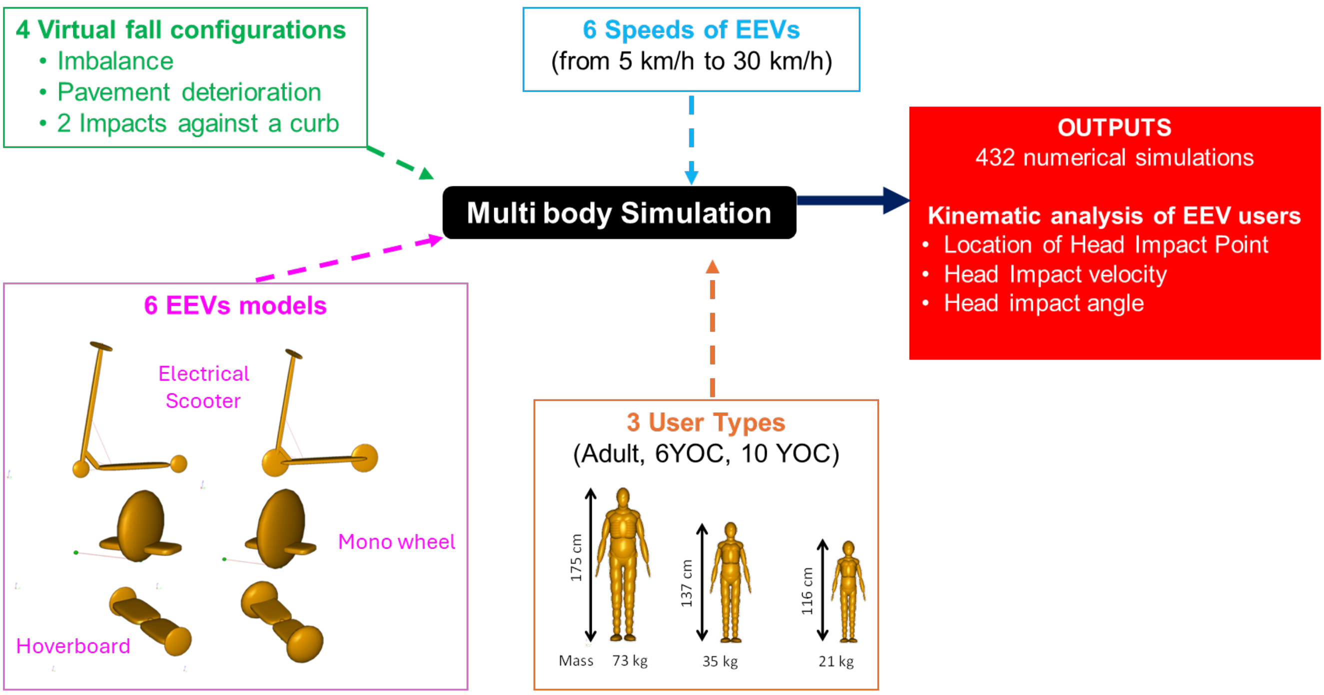

Fig. 3. Summary of parameters involved during multibody analysis of virtual accidents involving EEVs leading to a total of 432 multibody simulations.

Head trauma simulations and Helmet benefits

Following the kinematic analysis of EEV users during virtual fall simulations, head trauma and injury risk assessment will be conducted using a FE head model capable of predicting skull fractures and loss of consciousness. This section focuses on the model-based brain injury criteria established at Strasbourg University as well as the methodology used to quantify helmet-wearing benefits.

The SUFEHM is a numerical representation of the human head that incorporates realistic material properties for the brain and skull [18-22]. This model enables the computation of the brain's mechanical response to impact. To ensure anatomical accuracy, the inner and outer surfaces of the skull were digitised from an adult male human skull. The main anatomical components include the brain, brainstem, skin, and cerebrospinal fluid (CSF), represented by brick elements, while the skull, face, and two membranes, the falx and the tentorium are modelled using shell elements. SUFEHM consists of a continuous mesh with 13,208 elements, including 1,797 shell elements composing the skull and 5,320 brick elements for the brain. The total mass of the head model is 4.7 kg.

Each part of the SUFEHM, except for the brain and skull, is assigned isotropic, homogeneous, and elastic material properties. The brain is modelled using a linear isotropic viscoelastic law, with mechanical parameters derived from experimental data on human brain tissue [23] and *in vivo* values obtained from Magnetic Resonance Elastography (MRE) [24]. The model's validation was performed by [18-19] against local brain motion data [25-26] and intracranial pressure data [27-28].

The skull is modelled as a composite structure incorporating fracture mechanics [19]. It consists of a three-layered composite shell representing the inner table, diploë, and outer table of the cranial bone, with the diploë layer measuring 3 mm thick and the two cortical layers each measuring 2 mm. Various parametric studies were conducted to assess the robustness of the skull model, as reported in [20].

The proposed head model meets state-of-the-art standards in terms of stability and validation [19-21] [25-28] and has been used to establish tolerance limits for specific injury mechanisms. The primary objective was to develop robust and accurate injury criteria for predicting skull fractures and moderate diffuse axonal injuries (DAI, also referred to as concussions, AIS2+). To achieve this, real-world head trauma cases were reconstructed using existing accident databases, covering pedestrian, cyclist, motorsport, American football, and motorcycle accidents. The mechanical responses of the skull and brain during these incidents were analysed and correlated with actual injuries, allowing for the derivation of injury criteria for specific trauma mechanisms. A total of 85 well-documented head trauma cases were numerically reconstructed to develop a skull fracture injury risk curve. The proposed tolerance limit for a 50% risk of skull fracture was associated with 453 mJ of internal skull energy, as calculated using the head model [18]. Additionally, 109 real-world head trauma cases were simulated to develop robust brain injury criterion based on intracerebral von Mises stress to predict moderate DAI or short-term coma. The modelling was performed in accordance with the victim's kinematic analysis. Through an in-depth statistical analysis of various intracerebral parameters, von Mises stress was identified as the most reliable metric for predicting moderate DAI. The proposed brain injury tolerance limit for a 50% risk of moderate DAI, which corresponds to a reversible brain injury leading to loss of consciousness (AIS2+), was established at 36 kPa [29-30].

A detailed illustration of SUFEHM's different components as well as Injury risk curves predicting skull fracture probability (based on skull strain energy) and moderate brain injury (based on brain von Mises stress) are illustrated in Fig. 3.

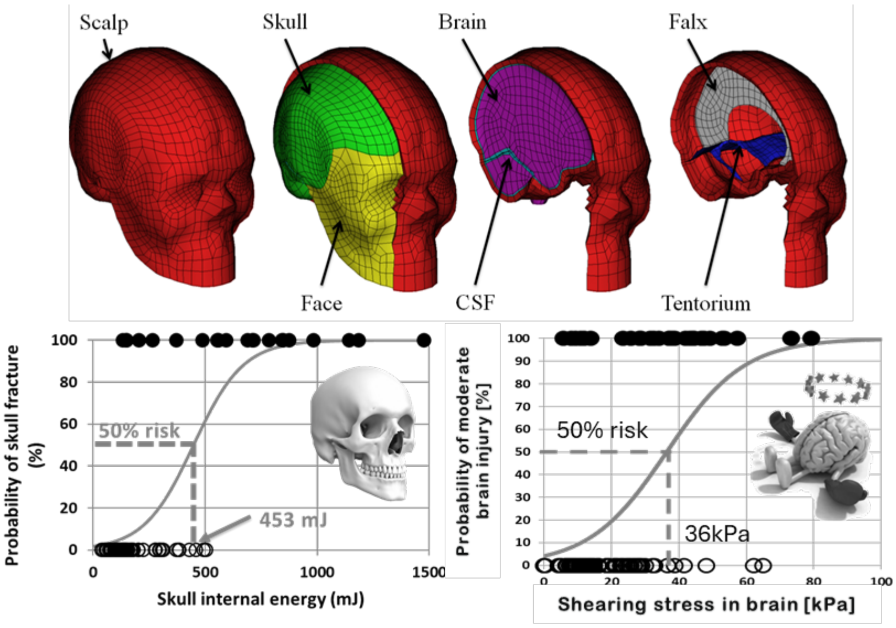

Fig. 3. Illustration of the different parts of the Strasbourg University Finite Element Head Model (SUFEHM), and injury risk curves to predict probability of skull fracture by addressing skull strain energy and to predict moderate reversible brain injury by addressing brain von Mises stress.

To assess head injury risks and to quantify the benefits of wearing a helmet, head trauma simulations were conducted both with and without a helmet. The FE bicycle helmet model used in this study is representative of a commercially available bicycle helmet, validated under both linear and oblique impact conditions [32]. The SUFEHM model, with and without helmet coupling, was oriented according to the conditions identified in fall simulations performed using multibody dynamics. The system then impacted the ground with boundary conditions extracted from MADYMO simulations. The finite element model of the ground used in this study comprises two layers: a 40 mm-thick subbase and an 80 mm-thick asphalt surface. The model is discretized using 19,200 solid 8-node elements with a uniform side length of 10 mm. Both materials are modelled using a linear elastic constitutive law. The mechanical properties implemented in LS-DYNA are as follows: for the subbase, a Young's modulus of 5.4 GPa; for the asphalt, 9.3 GPa. In both cases, the Poisson's ratio is set to 0.35 and the density to 1600 kg/m^3. CONTACT_AUTOMATIC_SURFACE_TO_SURFACE interfaces were implemented in LS-DYNA at various levels with a static friction coefficient of 0.7 for the head–ground and helmet–ground contacts under dry surface conditions, and a coefficient of 0.3 for the head–helmet contact.

In all head trauma simulations (both with and without a helmet), the risk of skull fracture and brain injuries was assessed by calculating the maximum skull strain energy and the maximum brain von Mises stress, respectively. The protective benefits of helmet use were further evaluated by comparing the results across all configurations. Figure 4 proposes an illustration of the methodology used to assess head injury risks with and without wearing a bicycle helmet.

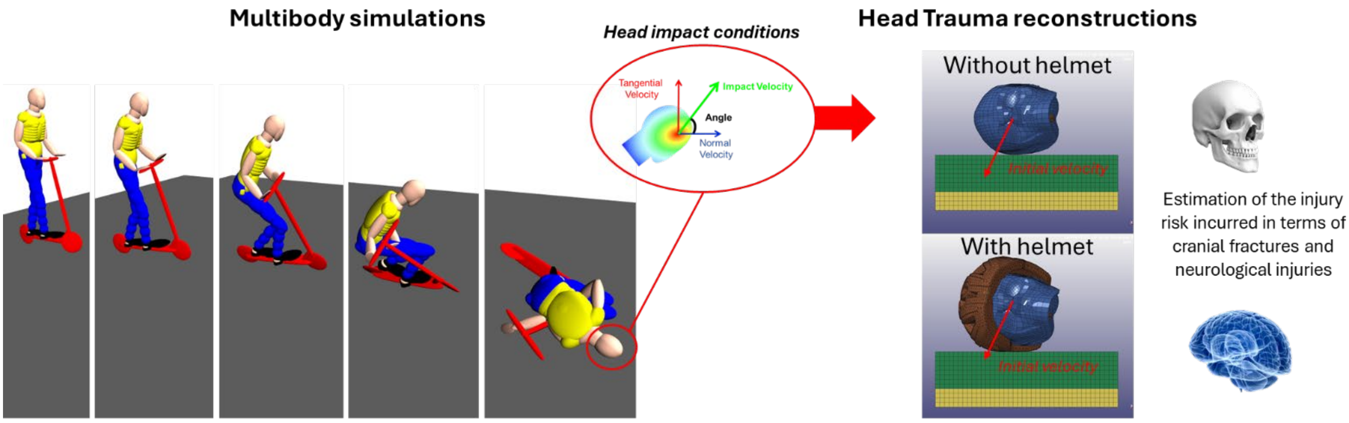

Fig. 4. Illustration of the methodology used to assess head injury risks with and without wearing a bicycle helmet.

III. RESULTS

A total of 432 multibody simulations were conducted. For each simulation, the head impact conditions just before ground contact, including impact speeds and angles, were extracted and analysed. Figure 5 illustrates a fall scenario involving a 10-year-old child caused by road surface deterioration (presence of a hole). The e-scooter's initial speed is 20 km/h, leading to a resultant head impact speed of 6.4 m/s (23 km/h) just before ground contact. The normal and tangential components of the impact speed are 5.7 m/s (20 km/h) and 2.8 m/s (10 km/h), respectively. Figure 6 illustrates the fall kinematics of an adult on a handlebar-less gyropod with 10" wheel size under different fall conditions.

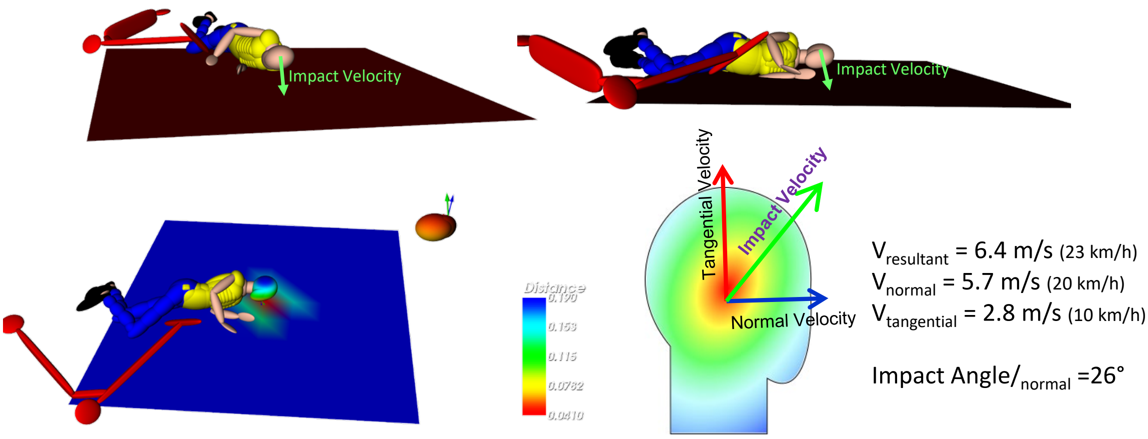

Fig. 5. Illustration of the head impact conditions as well as the speed vector for the case of a 10-year-old child falling due to a hole, with velocity at 20 km/h.

When considering all types of EEV and user profile, 48% of the impacts occur on the face. The remaining impacts are distributed across the frontal (19%), lateral (16%), and occipital (14%) regions (Figure 7a).

Analysing the results by user type (Figure 7b), it was observed that in 75% of the simulations, across all configurations, the resultant impact speed exceeds 5.1 m/s (18 km/h), and the normal impact speed is greater than 4.1 m/s (15 km/h). The speed levels are similar between 6-year-old and 10-year-old children, although impacts tend to be more tangential for younger children compared to adults. Across all simulations, the highest impact speeds are mainly recorded on the face and temporal region. On average (± standard deviation), the resultant impact speed on the face is 8.0 ± 1.7 m/s (29 ± 6 km/h), whereas in the frontal, lateral, and occipital regions it is around 5.4 m/s (19 km/h). The average impact angle is approximately 30°.

The analysis of different fall types (Figure 7c) indicates that head impact speeds are lower in cases of rear imbalance than in other scenarios. In 75% of simulations, the impact speed ranges from 4.8 m/s to 6.5 m/s for rear imbalance, whereas it ranges from 5.2 m/s to 8.4 m/s in falls caused by pavement deterioration, and from 5.4 m/s to 8.8 m/s in curb-impact scenarios under two different incidence angles.

Regarding the analysis by EEV type (Figure 7d), e-scooters result in lower-speed head impacts. In 50% of simulations, the impact speed is below 5.7 m/s (20.5 km/h), while for the handlebar-less gyropod and electric single-wheel the impact speeds exceed 7.1 m/s (25.5 km/h). For all these vehicles, the head–ground impact angle falls between 20° and 45° in 75% of cases.

The distribution of head impact locations also varies depending on the EEV type used. For e-scooter users, head impacts are more evenly distributed across the lateral (35%), facial (34%), and frontal (24%) regions. In contrast, for electric single-wheel and gyropod users, head impacts occur mainly on the face (50–60%) and the occipital region (25%).

Finally, the influence of EEV speed on head impact dynamics was analysed (Figure 7e). The results indicate that the resultant head impact speed increases with vehicle speed. The head impact velocity is greater than the speed of electric vehicle involved. However, the normal impact speed remains relatively stable in 50% of simulations, ranging between 4.7 m/s (15.2 km/h) and 6.6 m/s (19.4 km/h). In contrast, the tangential impact speed varies significantly, ranging from 1.5 m/s (3.8 km/h) to 7.5 m/s (24.7 km/h). When the EEV speed reaches or exceeds 25 km/h, the tangential component becomes more significant than the normal component. Lastly, at speeds above 10 km/h, the face, particularly the chin region, becomes the most frequently impacted area.

The key outputs here were head orientation and velocity before ground impact. Subsequently, head injury risks were assessed by simulating ground impacts with a FE model of the human head, with and without helmet protection.

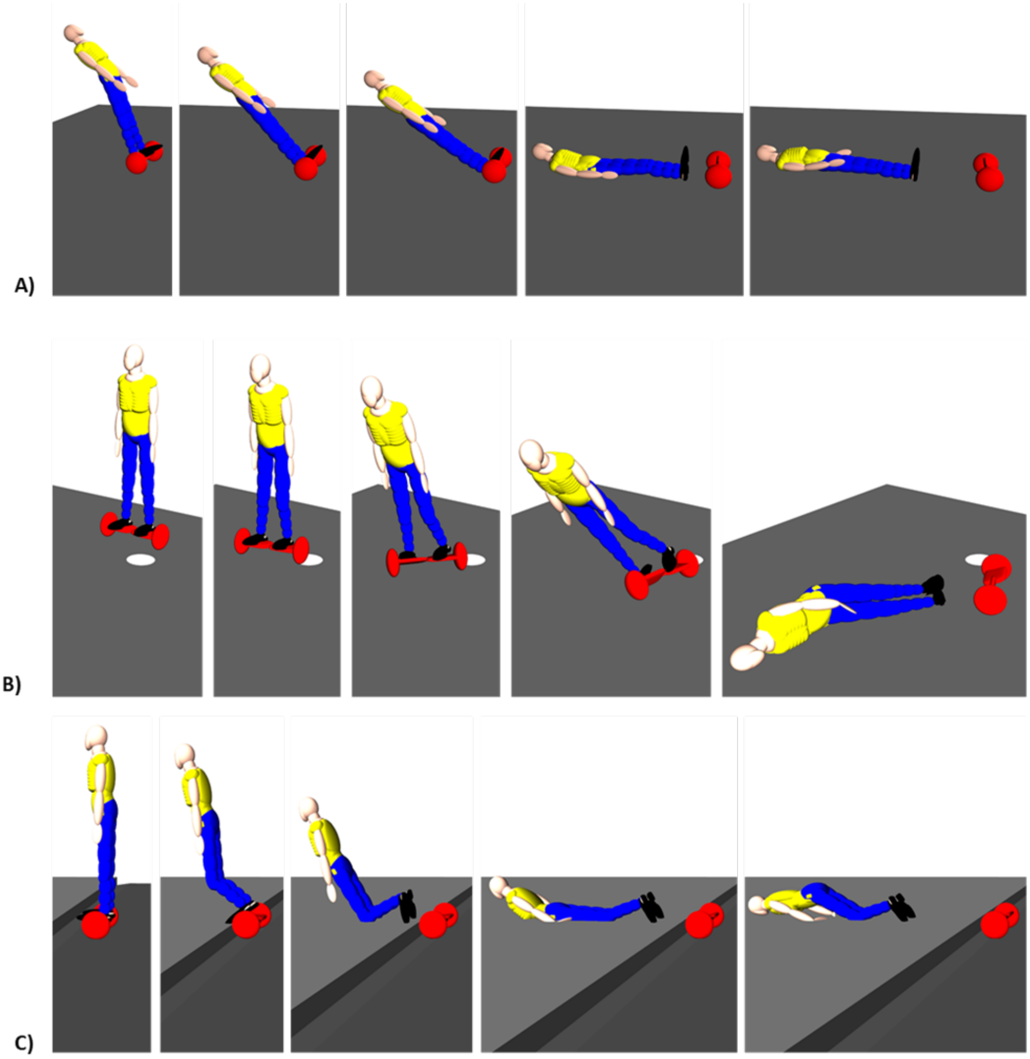

Fig. 6. Illustration of the fall kinematics of an adult on a handlebar-less gyropod with 10" wheel size: A) losing balance backward at 10 km/h; B) riding over a hole at 10 km/h; C) riding and impacting a curb at 10 km/h with a 90° incidence angle.

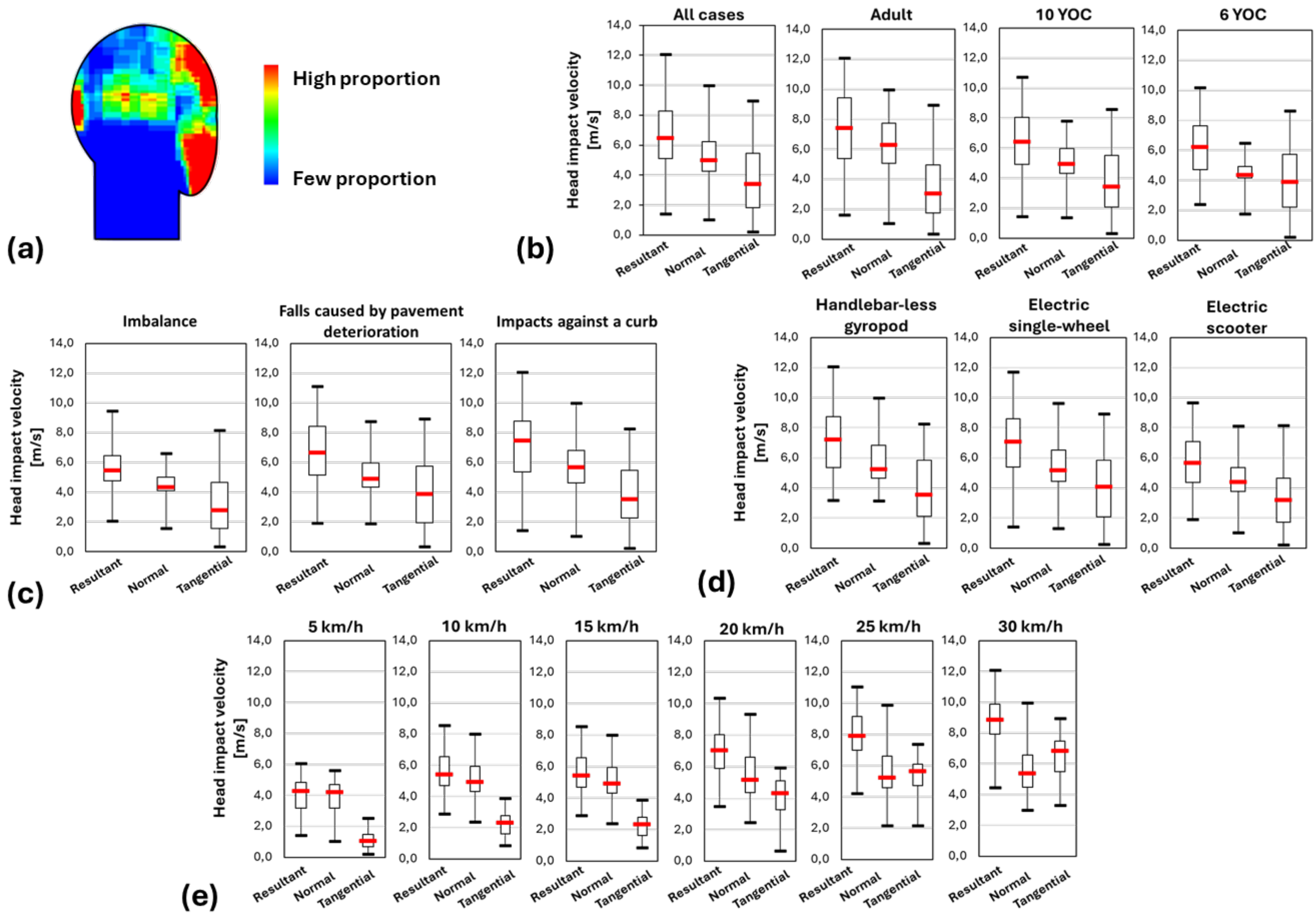

Fig. 7. (a) Distribution of head impact velocities from all 432 multibody simulations, regardless of user type and EEV category. (b) Boxplot of head-to-ground impact velocities by user type, aggregated across all EEV types and fall scenarios. (c) Boxplot of head-to-ground impact velocities according to the cause of the fall. (d) Boxplot of head-to-ground impact velocities by EEV category. (e) Boxplot of head-to-ground impact velocities as a function of EEV speed, across all vehicle types.

Out of the 432 virtual falls analysed, 221 impact conditions were selected for head trauma simulations using the SUFEHM, excluding all facial impacts. All facial impacts were excluded from the head trauma simulations, as the SUFEHM model features a simplified, rigid facial structure. This design choice ensures a coherent representation of the head's overall mass, inertia, and center of gravity, but limits the model's ability to accurately capture facial impact dynamics. The results, presented in Table I, highlight a high risk of injury when using EEVs without protection, both in terms of skull fractures and neurological injuries. The risk of skull fracture is particularly high: in 90% of reconstructed head impact simulations, it exceeds 95%. This risk remains significant even at low speeds, regardless of the type of user.

Similarly, the risk of moderate neurological injury exceeds 50% in 90% of the simulations. On average, this risk rises above 90% when the EEV speed exceeds 20 km/h, regardless of the user profile.

In conclusion, using EEVs without protection presents a high risk of head trauma, including both skull fractures and neurological injuries.

The head trauma simulations performed with the SUFEHM coupled with a helmet (summarised in Table II) show a significant reduction in head injury risk compared to simulations without a helmet, with an approximately 65% decrease in skull fracture risk and a 75% reduction in neurological injury risk. In certain cases, however, the risk of skull fracture remains high when the impact occurs near the helmet's edge. Overall, the fracture risk remains below 50% for all EEV users, decreasing from an average of 95% ± 15% without a helmet to 32% ± 28% with a helmet, including all user types.

Regarding the risk of moderate neurological injury, it generally does not exceed 30% for helmeted EEV users. The average risk for adult decreases from 80% ± 25% without a helmet to 22% ± 18% with a helmet, underscoring the effectiveness of helmet use in preventing head trauma.

Table III presents the numerical results obtained in terms of head trauma risk from numerical head impact simulations (SUFEHM) for the different EEV types and helmeted and unhelmeted users. Again, skull fracture risks for unhelmeted riders are high for all EEVs types (more than 92%). These percentage risks could be divided by 2-3 by wearing a head protective system. And the same trend is observed for brain injury risks, with the effectiveness of wearing a helmet potentially dividing by 4 the percentage risk of brain injuries.

TABLE I
SYNTHESIS OF HEAD INJURIES INCURRED DURING EEV USERS' ACCIDENTS

Users	EEV Speed	Brain Injury Risk	Skull Fracture Risk
Adult	5 km/h	65% ± 30%	*88% ± 28%*
	10 km/h	*82% ± 19%*	***98% ± 8%***
	15 km/h	*86% ± 6%*	***100% ± 0%***
	20 km/h	***92% ± 7%***	***100% ± 0%***
	25 km/h	***96% ± 4%***	***100% ± 0%***
	30 km/h	***97% ± 2%***	***100% ± 0%***
10 YOC	5 km/h	64% ± 27%	***91% ± 23%***
	10 km/h	*81% ± 14%*	***96% ± 9%***
	15 km/h	*78% ± 24%*	***98% ± 5%***
	20 km/h	*86% ± 14%*	***96% ± 15%***
	25 km/h	***95% ± 4%***	***100% ± 0%***
	30 km/h	***93% ± 11%***	***100% ± 0%***
6 YOC	5 km/h	58% ± 24%	***91% ± 14%***
	10 km/h	*74% ± 14%*	***97% ± 5%***
	15 km/h	*79% ± 24%*	***98% ± 3%***
	20 km/h	***97% ± 3%***	***99% ± 2%***
	25 km/h	***96% ± 4%***	***99% ± 6%***
	30 km/h	***96% ± 7%***	***100% ± 0%***

TABLE II
SYNTHESIS OF THE RESULTS OBTAINED IN TERMS OF AVERAGE RISKS CALCULATED WITH THE HELMETED AND UNHELMETED SUFEHM FOR THE DIFFERENT TYPES OF USER

	Brain Injury Risk		Skull Fracture Risk	
	Unhelmeted	**Helmeted**	**Unhelmeted**	**Helmeted**
Adult	*80% ± 25%*	22% ± 18%	***95% ± 19%***	33% ± 27%
10 YOC	*79% ± 23%*	19% ± 17%	***95% ± 16%***	30% ± 26%
6 YOC	*80% ± 23%*	21% ± 16%	***96% ± 9%***	35% ± 29%

TABLE III
SYNTHESIS OF THE NUMERICAL RESULTS OBTAINED IN TERMS OF HEAD TRAUMA RISK FROM NUMERICAL HEAD IMPACT SIMULATIONS (SUFEHM) FOR THE DIFFERENT EEVS HELMETED AND UNHELMETED USERS

	Brain Injury Risk		Skull Fracture Risk	
	Unhelmeted	**Helmeted**	**Unhelmeted**	**Helmeted**
Gyropods	*87% ± 16%*	22% ± 18%	***99% ± 3%***	40% ± 28%
Mono-wheel	*80% ± 22%*	15% ± 5%	***96% ± 17%***	21% ± 11%
E-scooter	*73% ± 28%*	23% ± 19%	***92% ± 18%***	33% ± 33%

IV. DISCUSSION

In this study, three emerging modes of travel were considered: the handlebar-less gyropod, the single-wheel, and the electric scooter (e-scooter). Various virtual fall scenarios were analysed, including rear imbalance, falls caused by road surface irregularities, and impacts against curbs, with EEV speeds ranging from 5 km/h to 30 km/h. A total of 432 virtual accident simulations were conducted, allowing for the assessment of user falls under different conditions. For each simulation, head loading conditions – specifically impact velocities and angles just before ground contact – were extracted. Although this study focuses primarily on head impacts and injury risk assessment, head rotation prior to impact was included as an input parameter in the head trauma simulations—with and without a helmet. However, its influence was not specifically investigated, as it falls outside the main scope of this work. Future studies could explore in greater detail the effect of pre-impact head rotation on head injury outcomes. These data, obtained from multibody simulations, served as inputs for the FE model of the human head developed by the biomechanics team in Strasbourg. This model is particularly notable for its predictive capability regarding skull fractures and neurological injuries.

The study's main findings indicate that as EEV speed increases, so does the risk of injury. The likelihood of skull fracture is generally high, with over 90% of impact simulations showing a fracture risk greater than 95%, even at lower speeds. Similarly, the calculated risk of neurological injury exceeds 50% in 90% of the simulations. This risk rises above 90% on average when EEV speeds exceed 20 km/h, regardless of user type.

Some of the results obtained in this study are consistent with previous findings in the literature, despite differences in accident scenarios. For example, [9] reported a head–ground impact force of 13.2 ± 3.4 kN during e-scooter falls, which exceeds commonly accepted skull fracture thresholds—aligning with the high fracture risk observed in our simulations. Similarly, the reported head–ground impact speed of 6.3 ± 1.4 m/s corresponds closely with the values calculated in our study. Furthermore, [9] found that all e-scooter falls resulted in oblique head impacts, with an average impact angle of 65 ± 10°, which is consistent with the impact angles predicted by our multibody simulations.

However, several limitations must be acknowledged. First, the range of impact conditions analysed is not exhaustive and could include additional configurations, such as falls involving lateral imbalances, rotational dynamics, or interactions with other obstacles. Nevertheless, the selected scenarios represent a realistic and diverse set of kinematic conditions.

Second, the use of a multibody approach introduces simplifications compared to FE simulations, particularly in the way body deformations and internal stress distributions are modelled. This may impact the accuracy of injury risk predictions.

Third, the HBM assumes a passive response to falls, whereas real users would likely engage in avoidance reflexes, such as turning their heads or adjusting body posture to mitigate facial or direct head impacts. This could influence the actual severity and nature of injuries in real-life situations.

Fourth, the study used a specific FE model for protective equipment, but if a different helmet is used that could significantly alter the head injury risk calculations. Future research should consider integrating the effectiveness of various helmets, especially with new technologies, as well as accounting for user behaviour in accident scenarios, to refine injury risk assessments. Head impact conditions – specifically, impact velocity and location – along with head injury risk were studied using a non-active human model.

Finally, the SUFEHM model was used to simulate head injury risks for both the 6- and 10-year-old cases. The time course of cranial bone development reveals several critical stages. Around the age of six, the child's head can generally be considered a scaled-down version of the adult head. Beyond this age, anatomical features such as the closure of fontanels and cranial sutures, along with the emergence of the diploë, gradually differentiate the pediatric skull from its adult counterpart. In future studies, once available, age-specific finite element models (e.g., a dedicated 6-year-old child head model) could be used to more accurately assess pediatric head injury risks.

Despite its limitations, this research provides valuable insights into the risks associated with EEVs and emphasises the importance of safety measures to mitigate head injuries.

V. CONCLUSION

This study highlights the significant risk of head trauma for EEV users during falls when no protective equipment, such as helmets, is worn. These risks include a high probability of skull fractures and neurological injuries. By quantifying these risks before accidents occur, the findings aim to provide valuable insights for public authorities and raise awareness among users. This analysis underscores the importance of considering mandatory helmet use for EEV riders and initiating discussions about the development of new helmet designs and the updating of safety standards tailored to these emerging modes of urban transport.

VI. ACKNOWLEDGEMENTS

The authors wish to thank the MechaniCS platform at the ICube Laboratory, Strasbourg University, as well as the French Ministry of the Interior, particularly the Road Safety Delegation (ONISR), for their invaluable support.

VII. REFERENCES

[1] ONISR (2023) Road safety annual report in French.

[2] Hardt, C., Bogenberger, K. (2019) Usage of e-scooters in urban environments. *Transportation Research Procedia*, **37**: pp. 155–162.

[3] Laa, B., Leth, U. (2020) Survey of E-scooter users in Vienna: Who they are and how they ride. *Journal of Transport Geography*, **89**, Article 102874.

[4] Kazemzadeh, K., Haghani, M., Sprei, F. (2023) Electric scooter safety: An integrative review of evidence from transport and medical research domains. *Sustainable Cities and Society*, **89**, Article 104313.

[5] Bourdet, N., Deck, C., Carreira, R. P., Willinger, R. (2012) Head impact conditions in the case of cyclist falls. *Journal of Sports Engineering and Technology*, **226**(3/4): pp. 282–289.

[6] Wang, S., Qian, Y., Qu, X. (2014) Reconstruction of car-electric bicycle side collision based on PC-Crash. *Journal of Transportation Technologies*, **4**: pp. 355–364.

[7] Xu, J., Shang, S., *et al*. (2016) Are electric self-balancing scooters safe in vehicle crash accidents? *Accident Analysis & Prevention*, **87**: pp. 102–116.

[8] Wang, F., Huang, J., *et al.* (2022) Numerical investigation of the rider's head injury in typical single-electric self-balancing scooter accident scenarios. *Journal of The Royal Society Interface*, **19**: p. 20220495.

[9] Posiriusk, P., Baker, C., Ghajari, M. (2022) Computational prediction of head-ground impact kinematics in e-scooter falls. *Accident Analysis & Prevention*, **167**, Article 106567.

[10] Ptak, M., Fernandes, F. A. O., *et al*. (2022) Analysis of electric scooter user kinematics after a crash against SUV. PLoS One1, **17**(1): p. e0262682.

[11] Pérez-Zuriaga, A. M., Dols, J., Nespereira, M., García, A., Sajurjo-de-No, A. (2023) Analysis of the consequences of car to micromobility user side impact crashes. *Journal of Safety Research*, **87**: pp. 168–175.

[12] Wei, W., Petit, Y., Arnoux, P. J., Bailly, N. (2023) Head-ground impact conditions and helmet performance in E-scooter falls. *Accident Analysis & Prevention*, **181**: 106935.

[13] Fournier, M., Bailly, N., Schäuble, A., Petit, Y. (2023) Head impact kinematics and injury risks during E-scooter collisions against a curb. *Heliyon*, **9**(9): e19254.

[14] Van Hoof, J., De Lange, R., Wismans, J. S. H. M. (2003) Improving Pedestrian Safety Using Numerical Human Models. *Stapp Car Crash Journal*, **47**: pp. 401–436.

[15] Robbins, D., Schneider, L., *et al*. (1983) Seated Posture of Vehicle Occupants. SAE Technical Paper 831617.

[16] Baughman, L. D. (1983) Development of an interactive computer program to produce body description data. AFAMRL-TR-83-058, 1983.

[17] Cheng, H., Obergefell, L., Rizer, A. (1994) Generator of body data (GEBOD) manual (Final Report, Apr. 1991–Mar. 1994).

[18] Deck, C., Willinger, R. (2009) Head injury prediction tool for predictive systems optimization. 7th European LS-DYNA Conference, 2008, Salzburg, Austria.

[19] Sahoo, D., Deck, C., Yoganandan, N., Willinger, R. (2013) Anisotropic composite human skull model and skull fracture validation against temporo-parietal skull fracture. *Journal of the Mechanical Behavior of Biomedical*

Materials, **28**: pp. 340–353.
[20] Sahoo, D., Deck, C., Yoganandan, N., Willinger, R. (2015) Influence of stiffness and shape of contact surface on skull fractures and biomechanical metrics of the human head of different population under lateral impacts. *Accident Analysis & Prevention*, **80**: pp. 97–105.
[21] Sahoo, D., Deck, C., Yoganandan, N., Willinger, R. (2015) Influence of head mass on temporo-parietal skull impact using finite element modelling. *Medical & Biological Engineering & Computing*, **53**: pp: 869–878.
[22] Sahoo, D., Deck, C., Yoganandan, N., Willinger, R. (2016) Development of skull fracture criterion based on real world head trauma simulations using finite element head model. *Journal of the Mechanical Behavior of Biomedical Materials*, **57**: pp. 24–41.
[23] Shuck, L. Z., Advani, S. H. (1972) Rheological response of human brain tissue in shearing. ASME *The Journal of Biomechanical Engineering*, pp. 905–911.
[24] Kruse, S. A., Rose, G. H., *et al.* (2007) Magnetic resonance elastography of the brain. *NeuroImage*, **39**: pp. 231–237.
[25] Hardy, W., Foster, C., *et al.* (2001) Investigation of head injury mechanisms using neutral density technology and high speed biplanar x-ray. *Stapp Car Crash Journal*, **45**: pp. 337–368.
[26] Hardy, W. N., Mason, M. J., *et al*. (2007) A study of the response of the human cadaver head to impact. *Stapp Car Crash Journal*, **51**: pp. 17–80.
[27] Nahum, A., Smith, R., and Ward, C. (1977). Intracranial pressure dynamics during head impact. Stapp Car Crash Journal, 21: pp. 336-339.
[28] Trosseille, X., Tarrière, C., Lavaste, F., Guillon, F. and Domont, A. (1992) Development of a FEM of the human head according to a specific test protocol. Proc. Of the 36th STAPP Car Crash Conference, SAE 922527, pp.235-253.
[29] Deck, C., Bourdet, N., Trog Arnaud, Meyer, F., Noblet Vincent & Willinger, R (2022). Deep learning method to assess brain injury risk. International Journal of Crashworthiness, DOI: 10.1080/13588265.2022.2130600.
[30] Deck, C., Bourdet, N., Meyer, F., & Willinger, R. (2019). Protection performance of bicycle helmets. Journal of Safety Research, 71, 67–77. https://doi.org/10.1016/j.jsr.2019.09.003.
[31] Burke A. M., Olatunbosun O. A., (1997), Static Tyre/Road Interaction Modelling, Meccanica, 32, (5): pp. 473 479, doi: 10.1023/A:1004264018606.
[32] Milne, G., Deck, C., Bourdet, N., Carreira, R. P., Allinne, Q., Gallego, A., & Willinger, R. (2013). Bicycle helmet modelling and validation under linear and tangential impacts. International Journal of Crashworthiness, 19(4): pp. 323–333.